IEEE Access
Multidisciplinary ⋮ Rapid Review ⋮ Open Access Journal

Received June 14, 2020, accepted June 28, 2020, date of publication July 1, 2020, date of current version July 13, 2020.

Digital Object Identifier 10.1109/ACCESS.2020.3006203

Bottom-Following Control of Underactuated Unmanned Undersea Vehicles With Input Saturation

HAOMIAO YU, CHEN GUO, YANAN HAN, AND ZHIPENG SHEN
College of Marine Electrical Engineering, Dalian Maritime University, Dalian 112016, China

Corresponding authors: Haomiao Yu (yuhaomiao1983@163.com) and Chen Guo (guoc@dlmu.edu.cn)

This work was supported in part by the National Natural Science Foundation of China under Grant 51809028, Grant 51879027, and Grant 51579024, in part by the Doctoral Start-Up Foundation of Liaoning Province under Grant 2019-BS-022, and in part by the Fundamental Research Funds for the Central Universities under Grant 3132019318.

ABSTRACT This article addresses the subject for bottom-following control of underactuated unmanned undersea vehicles (UUVs) with input saturation in the presence of unknown model uncertainties and unknown external disturbances. A robust adaptive dynamic surface bottom-following control scheme is developed based on the recursive sliding mode with nonlinear gains and neural networks, which can steer an underactuated UUV to precisely follow the bottom profile at a constant altitude as a basic feature. The bottom-following guidance law is derived based on the Serret-Frenet frame, the line of sight (LOS) and Lyapunov's direct technique. Then, the bottom-following controller is designed based on the recursive sliding mode and dynamic surface control (DSC), to stabilize the bottom-following errors. The radial basis function neural networks (RBF NNs) are employed to online approximate the uncertain dynamics of underactuated UUVs, while the adaptive laws are introduced to estimate the bounds of the RBF NN approximation errors and unknown environmental disturbances. Additionally, an auxiliary dynamic system (ADS) is presented to handle the effect of input saturation. The uniform boundedness of all the closed-loop signals is guaranteed via Lyapunov analysis. The simulation results are presented to verify and illustrate the effectiveness of the proposed control scheme.

INDEX TERMS Underactuated unmanned undersea vehicle, bottom-following, recursive sliding mode, input saturation, model uncertainties.

I. INTRODUCTION

Unmanned undersea vehicles (UUVs) have be used for a broad range of marine scientific, marine commercial and marine military applications [1]–[4], as they can perform the dull, dirty and dangerous tasks (3D tasks). Nowadays, UUVs are mainly applied to seafloor mapping, ocean survey, submarine pipeline inspection, exploration and exploitation of resources, undersea search, etc. [1]. The bottom-following is a typical motion control problem of underactuated UUVs, which is concerned with the design of control strategies that steer an UUV to sail on such a desired path relies on the bottom terrain at a constant altitude. In practical engineering, the reference path for the bottom-following is planned online by fitting the measurement information of the seabed terrain to the task requirements. Then, the underactuated UUV is driven by the bottom-following controller, to track the reference path. In this work, a solution to the problem of the bottom-following control for underactuated UUVs is presented.

The motion control actuators of UUVs, considering propulsion efficiency, cost and displacement, are usually set to underactuated mode, that is, the number of the actuators is less than degrees of freedom (DOF). For the bottom-following control problem of underactuated UUVs, it is essential that the efficient and robust motion controller is developed to force them to follow the seabed profile at a constant altitude as a basic feature. However, the bottom-following control of underactuated UUVs faces huge challenges such as second-order nonholonomic constraints with drift items, model uncertainties, unknown ocean currents, and input saturation [5], [6].

The associate editor coordinating the review of this manuscript and approving it for publication was Fanbiao Li.

In view of the demand for the precise motion-control of underactuated UUVs in practical application, scholars devoted themselves to study this topic in recent decades. For underactuated UUVs, motion controllers are developed based on the following controller-design methods, including backstepping technique [7]–[9], sliding mode control (SMC) [5]–[7], [10]–[14], adaptive control [8], [15]–[19], neural network [19]–[24], fuzzy logic control (FLC) [25]–[27]. To ensure UUV sailing at a constant altitude from the seabed, several related literatures have been published [13], [14], [28], [29]. The bottom-following problem for the INFANTE AUV was transformed into the stabilized problem of a discrete-time error space dynamics, and then the preview controller based on the linear matrix inequalities and D-methodology was designed to stabilize it [28]. The bottom-following problem of underactuated AUVs was given a solution based on the nonlinear iterative sliding mode [14]. For a low cost UUV, the output feedback controller based on nonlinear output regulation theory and Fourier series theory was developed to solve the bottom-following problem [29]. Yan *et al.* proposed a robust bottom-following controller using integral-terminal sliding mode control (ITSMC), which steers the under-actuated UUV to follow the bottom profile at a constant altitude as a basic feature [13].

For the aforementioned control schemes, the dynamics of underactuated UUVs must be accurate or that there is only parameter perturbation with known supremum, while all bottom-following controllers are based on the assumption of unconstrained motion-control actuators. However, an accurate dynamic model cannot be obtained in practice to parameter perturbations and high-order unmolded dynamics. For a practical perspective, any motion control actuators of UUVs cannot implement unlimited force or moment due physical constraints, namely input saturation. Therefore, the performance of the bottom-following control does not satisfy in presence of non-accurate models and input saturation, based on the above-mentioned control strategies. Sliding mode control is widely applied to solve the problem of controller-design for various nonlinear systems, which can deal with control problems under model uncertainties, disturbances and so on [30]–[32]. Therefore, SMC-class controllers are also widely used for the motion control of underactuated UUVs.

Inspired by the above considerations, this work develops the adaptive RBF NN-DSC-based recursive sliding mode control scheme for the bottom-following of the underactuated UUV with uncertainties and input saturation. The bottom-following control scheme is made up two segments, including the bottom-following guidance law and dynamic controller. Based on the LOS and Lyapunov's direct technique, the guidance law is derived. Meanwhile, the dynamic controller is developed by using the recursive sliding mode with nonlinear gains and neural networks. The RBF NNs are applied to online approximate the uncertain dynamics of underactuated UUVs, while the adaptive laws are introduced to estimate the bounds of the RBF NN approximation errors and unknown environmental disturbances. Additionally, an auxiliary dynamic system (ADS) is presented to handle the effect of input saturation. It is known that all the closed-loop signals are uniform boundedness via Lyapunov analysis.

This approach is able to effectively solve the contradiction of possess high control accuracy and good transient performance at the same time in the presence of input saturation and the designed controller is non-fragile to the perturbation of its own parameters. The main contributions of this work are summarized as follows:

(1) This work proposes a robust adaptive RBF-NN-DSC bottom-following control scheme using ''small-error large-gain and large-error small-gain'' idea, which can deal with the balance between the control gain and performance.

(2) The recursive sliding mode with nonlinear gains is developed to the dynamic controller to deal with the parameter perturbation caused by DSC.

(3) The RBF NN technique is applied to online approximate the model un unknown model uncertainties and unknown external disturbances, which can enhance the robustness of the proposed bottom-following controller.

The organization of this paper is as follows. Section II presents the kinematics and dynamics of underactuated UUVs and problem formulation. In section III, the bottom-following guidance law is developed based the LOS and Lyapunov's direct technique. The dynamic controller is designed based the adaptive RBF NN-DSC-based recursive sliding mode in section IV. Section V provides the numerical simulation results and analysis, which validate the effectiveness and robustness of the proposed controller. In section VI, brief conclusions are drawn.

II. PROBLEM FORMULATION

A. UUV KINEMATICS AND DYNAMICS

In this section, the kinematics and dynamics of underactuated UUVs are presented, which can be described using the inertial coordinate frame $\{n\}$ and the body-fixed coordinate frame $\{b\}$, as shown in Fig.1. The research object is a neutrally buoyant UUV with three principal planes of symmetry. In view of this study is the bottom-following, the sway, yaw and roll motions of underactuated UUVs are negligible, namely $v = 0$, $y = 0$, $p = r = 0$ and $\phi = \psi = 0$. Then, the kinematic equations of underactuated UUVs in the vertical plane are written as follows [7], [13], [28], [29]

$$\begin{cases} \dot{x} = u\cos\theta + w\sin\theta \\ \dot{z} = -u\sin\theta + w\cos\theta \\ \dot{\theta} = q \end{cases} \tag{1}$$

where, x and z are the position coordinates of UUVs in $\{n\}$; θ is the pitch angle; u and w denote the surge and heave velocity in $\{b\}$; q represents the pitch angular velocity. For the bottom-following case, the surge velocity u can be assumed to be never equal zero. The angle of attack is equal to $\alpha = \arctan(w/u)$. To facilitate the design of the bottom-following

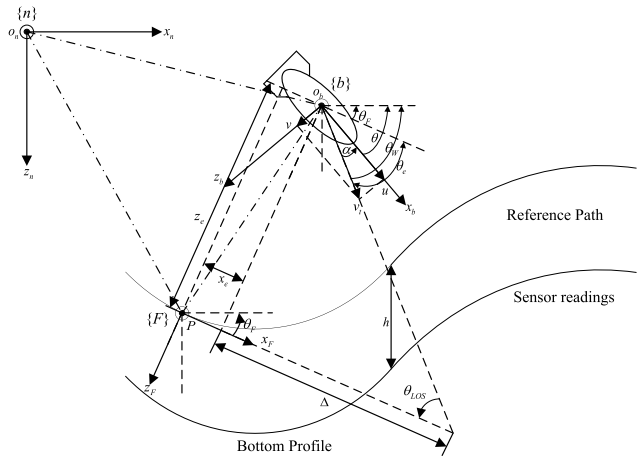

FIGURE 1. The bottom-following schematic of an underactuated UUV.

controller, the flow frame (FF) $\{W\}$ is introduced by rotating $\{b\}$ around the y_b-axis through α in the positive direction. Therefore, the kinematics can be described as [13]:

$$\begin{cases} \dot{x} = v_t \cos\theta_W \\ \dot{z} = -v_t \sin\theta_W \\ \dot{\theta}_W = q - \dot{\alpha} \end{cases} \tag{2}$$

where, $\theta_W = \theta - \alpha$; and v_t denotes the total speed of UUV, i.e., $v_t = \|v_t\| = \sqrt{u^2 + w^2}$.

For a practical UUV, its mass distribution is usually assumed to be homogeneous. To facilitate the design of the motion controller, the order of the hydrodynamic drag terms is lower than two. Considering the parameter perturbation, unmodeled dynamics and unknown external disturbances, the dynamics of underactuated UUVs in the vertical plane can be simplified as:

$$\begin{cases} m_{11}\dot{u} = -m_{22}wq - X_u u - X_{u|u|}u\,|u| + \tau_u + \Delta f_u \\ m_{22}\dot{w} = m_{11}uq - Z_w w - Z_{w|w|}w\,|w| + \Delta f_w \\ m_{33}\dot{q} = (m_{22} - m_{11})uw - M_q q - M_{q|q|}q\,|q| \\ -(z_G W - z_B B)\sin\theta + \tau_q + \Delta f_q \end{cases} \tag{3}$$

where, $m_{11} = m - X_{\dot{u}}$, $m_{22} = m - Z_{\dot{w}}$ and $m_{33} = I_y - M_{\dot{q}}$ are the combined inertia and added mass terms. $X_{\{\cdot\}}$, $Z_{\{\cdot\}}$ and $M_{\{\cdot\}}$ denote the hydrodynamic coefficients. Δf_u, Δf_w and Δf_q indicate the model uncertainties (including the parameter perturbation and unmodeled dynamics). W and B are the gravity and buoyancy of an underactuated UUV, and $B = W = mg$. z_G and z_B mean the z_b-component of the center of gravity and buoyancy in $\{b\}$, respectively. τ_u and τ_r are the input force and torque that are applied to the UUV, which exist inherent actuator saturation [33]. Therefore, these control inputs are presented below:

$$\tau_i = sat(\tau_i^c) = \begin{cases} \tau_i^{\max}, \tau_i^c \geq \tau_i^{\max} \\ \tau_i^c, \quad \tau_i^{\min} < \tau_i^c < \tau_i^{\max} \\ \tau_i^{\min}, \tau_i^c \leq \tau_i^{\min} \end{cases} \tag{4}$$

where, $i = u,\ q$. The term τ_i^c is the motion control signal. $\tau_i^{\max}$ and $\tau_i^{\min}$ denote the maximum and minimum applicable control signal, respectively.

Assumption 1: The velocity of underactuated UUV in heave direction is passive bounded in the sense that $\sup_{t\geq 0}|w| < \sigma_w$, where σ_w is a small positive constant.

Assumption 2: The external time-varying disturbance caused by wave and ocean current is bounded.

Assumption 3: The pitch angle of underactuated UUV satisfies $|\theta| < \sigma_\theta \leq 0.5\pi$, such that its pitch angle is bounded.

Assumption 4: The motion states of this underactuated UUV can be available for the feedback in real-time, including positon, pitch angle and surge velocity.

B. ERROR DYNAMIC EQUATIONS

The bottom-following controller should perform the below two objectives: 1) the origin o_b of $\{b\}$ coincides with the reference point P on the desired path, 2) the float angle θ_W of the UUV equals to the tangential angle at the reference point P. To achieve the aforementioned control objectives, the error dynamic equations should be constructed. To facilitate the construction of dynamic equations, a Serret-Frenet frame $\{F\}$ is introduced at the reference point P, which plays the role of a "virtual target vehicle".

The posture of the virtual target vehicle is expressed as $p_{\mathrm{R}} = [x_{\mathrm{R}}, z_{\mathrm{R}}, \theta_F]^{\mathrm{T}}$ in P. The reference point P is an arbitrary point on the desired path, which is stated by the curvilinear abscissa s. The posture errors p_e in $\{F\}$ is expressed as

$$p_e = \mathbf{R}_n^F(\theta_F)(\boldsymbol{p}_n - \boldsymbol{p}_{\mathrm{R}}) \tag{5}$$

where, $\boldsymbol{p}_e = [x_e, z_e, \theta_e]^{\mathrm{T}}$. θ_F denotes the rotation angle from $\{n\}$ to $\{F\}$, and its specific definition is as follows

$$\theta_F = \arctan\frac{z'_{\mathrm{R}}}{x'_{\mathrm{R}}} \tag{6}$$

The symbol $(\cdot)'$ indicates the first derivative of the corresponding variable with respect to the path parameter. The pitch angular velocity of the "virtual vehicle" is defined as

$$q_F = \dot{\theta}_F = \kappa(s)\dot{s} \tag{7}$$

where, $\kappa(s)$ is the path curvature at the reference point P. The rotation matrix $\mathbf{R}_n^F(\theta_F)$ from $\{n\}$ to $\{F\}$ is defined as

$$\mathbf{R}_n^F(\theta_F) = \begin{bmatrix} \cos\theta_F & -\sin\theta_F & 0 \\ \sin\theta_F & \cos\theta_F & 0 \\ 0 & 0 & 1 \end{bmatrix} \tag{8}$$

where, $\mathbf{R}_n^F(\theta_F) \in SO(3)$. $SO(3)$ denotes the third-order special orthogonal group. The rotation matrix $\mathbf{R}_n^F(\theta_F)$ satisfies the following condition:

$$\dot{\mathbf{R}}_n^F(\theta_F) = \mathbf{R}_n^F(\theta_F)\mathbf{S}(\theta_F)\dot{\theta}_F = \dot{\theta}_F\mathbf{S}(\theta_F)\mathbf{R}_n^F(\theta_F) \tag{9}$$

where the matrix $\mathbf{S}(\theta_F)$ is as follows

$$\mathbf{S}(\theta_F) = \begin{bmatrix} 0 & -1 & 0 \\ 1 & 0 & 0 \\ 0 & 0 & 0 \end{bmatrix}$$

Taking the time-derivative of the error equation (5), the dynamic equations regarding the posture errors are obtained

$$\begin{bmatrix} \dot{x}_e \\ \dot{z}_e \\ \dot{\theta}_e \end{bmatrix} = \begin{bmatrix} -\kappa(s)\dot{s}z_e + v_t\cos\theta_e - \dot{s} \\ \kappa(s)\dot{s}x_e - v_t\sin\theta_e \\ q - \dot{\alpha} - \kappa(s)\dot{s} \end{bmatrix} \tag{10}$$

C. CONTROL OBJECTIVES

For the bottom-following of the practical UUV, its control objectives can be formulated as follows:

Consider a sufficiently smooth reference path with a constant altitude, which can be obtained by fitting the measurement information of the seabed terrain to the task requirements. The underactuated UUV with the motion model (2) and (3) can be steered to the reference path under the designed bottom-following controller. In other words, the posture errors x_e, z_e and θ_e under the guidance laws β_u, β_s and β_q can converge to arbitrarily small neighborhoods of the origin, i.e.

$$\lim_{t\to\infty}|x - x_{\mathrm{R}}| \le \varepsilon_1, \quad \lim_{t\to\infty}|z - z_{\mathrm{R}}| \le \varepsilon_2, \quad \lim_{t\to\infty}|\theta - \theta_{\mathrm{R}}| \le \varepsilon_3$$

where, ε_1, ε_2 and ε_3 are arbitrarily small positive constants. Then, the following error variables are defined

$$\begin{bmatrix} u_e \\ q_e \end{bmatrix} = \begin{bmatrix} u - \beta_u \\ q - \beta_q \end{bmatrix} \tag{11}$$

Under the designed bottom-following controller, the velocity errors u_e and q_e are stabilized to arbitrarily small neighborhoods of the origin, i.e.

$$\lim_{t\to\infty}|u_e| \le \varepsilon_4, \quad \lim_{t\to\infty}|q_e| \le \varepsilon_5$$

where, ε_4 and ε_5 are arbitrarily small positive constants.

D. PRELIMINARIES

To improve the dynamic performance of the bottom-following controller, a continuously differentiable nonlinear gain function $\varpi(x)$ is developed as follows [34], [35]:

$$\varpi(x) = \begin{cases} x, & |x| \le \wp \\ \alpha(|x|^{0.5} - 0.25\alpha)\mathrm{sgn}(x), & |x| > \wp \end{cases} \tag{12}$$

where, α is a positive constant and $\wp = 0.25\alpha^2$. $\forall x \in \mathbb{R}$. The gain function $\varpi(x)$ satisfies the following properties:

Property 1: The gain function $\varpi(x)$ is strictly monotone increasing and continuously differentiable. The gain function $\varpi(x)$ reflects "small-error large-gain and large-error small-gain" idea.

Property 2: The first derivative of the gain function $\varpi(x)$ is as follows

$$\frac{d\varpi(x)}{dx} = \begin{cases} 1, & |x| \le \wp \\ \dfrac{\alpha}{2}|x|^{-0.5}, & |x| > \wp \end{cases} \tag{13}$$

The following nonlinear function is developed

$$L(x) = \frac{1}{2}\left[\frac{d\varpi(x)}{dx}x + \varpi(x)\right] \tag{14}$$

and it satisfies the following properties:

Property 3: The nonlinear function $L(x)$ is strictly increasing and satisfies following condition

$$x \times L(x) = \frac{1}{2}\left[\frac{d\varpi(x)}{dx}x^2 + x \times \varpi(x)\right] \ge \frac{1}{2}x \times \varpi(x) \tag{15}$$

Further, the third nonlinear function is defined as follows

$$N(x) = \begin{cases} 1, & |x| \le \wp \\ \dfrac{L(x)}{x}, & |x| > \wp \end{cases} \tag{16}$$

For any continuous function $f(x) : \mathbb{R}^n \to \mathbb{R}$ within a compact set $\Omega \subset \mathbb{R}^n$, it can be approximated with any arbitrary accuracy by the RBF NN [36], that is to say

$$f(\boldsymbol{x}) = \boldsymbol{W}^{*\mathrm{T}}\boldsymbol{h}(\boldsymbol{x}) + \varepsilon, \quad \forall x \in \Omega \tag{17}$$

where ε is the approximation error with an assumption $|\varepsilon| \le \varepsilon_M$. W^* denotes the ideal weight vector and is defined as the value of W that minimizes the that minimizes the deviation $|\varepsilon|$ for all $x \in \Omega$, that is

$$\boldsymbol{W}^* \triangleq \arg\min_{W\in\mathbb{R}^m}\left\{\sup_{x\in\Omega}\left|f(\boldsymbol{x}) - \boldsymbol{W}^{\mathrm{T}}\boldsymbol{h}(\boldsymbol{x})\right|\right\} \tag{18}$$

where $W^{\mathrm{T}}h(x)$ is the radial basis function neural network (RBF NN) and can approximate a continuous function $f_N(x)$ within a compact set $\Omega \subset \mathbb{R}^n$. $W = [w_1, \ldots, w_m]^m \in \mathbb{R}^m$ $(m > 1)$ is the weight vector of the RBF NNs, $x = [x_1, \ldots, x_n]^{\mathrm{T}} \in \Omega$ is the input vector, and $h(x) = [h_1(x), \ldots, h_m(x)]^{\mathrm{T}} \in \mathbb{R}^m$ is the basis function vector. $h_j(x)$ is the Gaussian kernel function as follows

$$h_j(x) = e^{-\frac{\|x-\mu_j\|^2}{2\sigma_j^2}}, \quad j = 1, \ldots, m \tag{19}$$

where $\mu_j = [\mu_{j,1}, \ldots, \mu_{j,n}]^{\mathrm{T}}$ is the center of the Gaussian kernel function and σ_j is the width of the Gaussian kernel function.

III. GUIDANCE LAW DESIGN

The guidance can continuously provide the desired surge velocity, pitch angular velocity and the change rate of the curvilinear abscissa s associated with the achievement of motion control objectives [7]. The input of the guidance law is the position coordinates of the reference path. The bottom-following guidance law is developed based on the line-of-sight (LOS) and the tracking differentiator [13], [37].

A. THE POSITION AND ATTITUDE GUIDANCE

The reference path of UUV for the bottom-following is parameterized by the curvilinear abscissa s with a globally defined update law [13], [17]. The bottom-following errors x_e, z_e and θ_e are well defined for each curvilinear abscissa s. Thus, the update law of the curvilinear abscissa s is set to an extra degree of freedom in the design of the motion controller.

Consider the Lyapunov function $V_{kin1} = (x_e^2 + z_e^2)/2$. Then, its first-order derivative with Eq. (10) can be calculated as

$$\dot{V}_{kin1} = x_e\dot{x}_e + z_e\dot{z}_e = v_t x_e \cos\theta_e - v_t z_e \sin\theta_e - \dot{s}x_e$$

The update law $\dot{s}$ is chosen as

$$\beta_s = \dot{s} = v_t \cos\theta_e + k_s x_e \tag{20}$$

where k_s is an adjustable positive gain parameter. Then, the first-order derivative $\dot{V}_{kin1}$ become

$$\dot{V}_{kin1} = -v_t z_e \sin\theta_e - k_s x_e^2 \tag{21}$$

Next, the attitude guidance is developed based on the LOS guidance principle [38]. The LOS approach angle is designed as follows [13]

$$\delta_\theta = \arcsin(\frac{k_\theta z_e}{\sqrt{z_e^2 + \Delta^2}}) \tag{22}$$

where k_θ is an positive gain parameter. $\Delta = 2l - lsat(k_c\,|\kappa(s)|)$, where $k_c > 0$, $sat(\cdot)$ denotes saturation function, and$l$is the vehicle total length. The LOS approach angle is instrumental in shaping transient maneuvers during the path approach phase [17].

Theorem 1: Consider the kinematic model of an underactuated UUV described in Eq. (2) and the dynamic equations regarding the posture errors described in Eq. (10). The position and attitude guidance is designed as follows

$$\begin{cases} \beta_s = v_t \cos\theta_e + k_s x_e \\ \beta_q = \dot{\alpha} + \kappa(s)\dot{s} + \dot{\delta}_\theta - k_1^q L(\theta_e - \delta_\theta) \end{cases} \tag{23}$$

so that the posture errors can be guaranteed to converge to a specified compact set around the origin. k_1^q is an adjustable positive gain parameter.

Proof: The sliding mode surface with respect to the pitch angle error is defined as follows:

$$S_1 = \theta_e - \delta_\theta \tag{24}$$

Its first time-derivative according to Eq. (10) is obtained as follows

$$\dot{S}_1 = \dot{\theta}_e - \dot{\delta}_\theta = q - \dot{\alpha} - \kappa(s)\dot{s} - \dot{\delta}_\theta \tag{25}$$

To analyze the convergence of the pitch angle error, the Lyapunov function is chosen as follows

$$V_{kin2} = \frac{1}{2} S_1 \varpi(S_1) \tag{26}$$

Obviously, the Lyapunov function V_{kin2} is positive definite. Then, its first-order derivative is calculated as

$$\begin{aligned} \dot{V}_{kin2} &= \frac{1}{2}\dot{S}_1(\varpi(S_1) + \frac{d\varpi(S_1)}{dS_1}S_1) \\ &= (q - \dot{\alpha} - \kappa(s)\dot{s} - \dot{\delta}_\theta)L(S_1) \end{aligned} \tag{27}$$

It is straightforward to indicate that the desired pitch angular velocity

$$\beta_q = \dot{\alpha} + \kappa(s)\dot{s} + \dot{\delta}_\theta - k_1^q L(S_1) \tag{28}$$

makes $\dot{V}_{kin2} = -k_1^q L(\theta_e - \delta_\theta)^2 \leq 0$. Therefore, the Lyapunov function $\dot{V}_{kin2}$ is a positive definite and monotonically decreasing function up to a well-defined limit

$$\lim_{t\to\infty} V_{kin2} = \gamma_0 \tag{29}$$

Its second-order derivative $\ddot{V}_{kin2}$ can be calculated as

$$\ddot{V}_{kin2} = 2k_q L(S_1)^2 \frac{dL(S_1)}{dS_1} \tag{30}$$

Based on Corollary of Barbalat's Lemma (CBL) [13], the following results can be obtained

$$\lim_{t\to 0} \dot{V}_{kin2}(t) = 0$$

That is

$$\lim_{t\to 0} \theta_e = \delta_\theta|_{t\to 0} \tag{31}$$

The motion system of an underactuated UUV can asymptotically follow the desired pitch angler error defined in Eq.(22). Therefore, the trajectories of the UUV system are asymptotically converging to an invariant set

$$\{\Omega_{nav}|(x_e, z_e) \in \mathbb{R}^2, \theta_e = \delta_\theta\} \tag{32}$$

Next, the convergence of the position errors is analyzed. When the trajectories of the UUV system converge to the invariant set Ω_{nav}, the pitch angle error θ_e equals δ_θ. Then, the first-order derivative $\dot{V}_{kin1}$ satisfies the following conditions

$$\begin{aligned} \dot{V}_{kin1} &= -v_t z_e \sin\theta_e - k_s x_e^2 = -k_\theta \frac{v_t z_e^2}{\sqrt{z_e^2 + \Delta^2}} - k_s x_e^2 \\ &\leq -2\min(k_\theta \frac{v_t}{\sqrt{z_e^2 + \Delta^2}}, k_s) V_{kin1} \leq 0 \end{aligned} \tag{33}$$

Similarly, the Lyapunov function V_{kin1} is bounded. Moreover, it is straightforward to show that $\ddot{V}_{kin1}$ is also finite. Then, the CBL indicates for the conclusion that $\lim_{t\to\infty} \dot{V}_{kin1} = 0$. which implies $\lim_{t\to\infty} x_e(t) = 0$ and $\lim_{t\to\infty} z_e(t) = 0$ ($(x_e, z_e) = (0, 0)$is the unique equilibrium point in the set Ω_{nav}). From the definition (22), $\lim_{t\to\infty} z_e(t) = 0$ indicates $\lim_{t\to\infty} \theta_e = \lim_{t\to\infty} \theta_{LOS} = 0$ within Ω_{nav}. Wherefore, all trajectories of the underactuated UUV can asymptotically converge to an invariant set

$$\{\Omega_{path}|(x_e, z_e) = \mathbf{0}^2\} \tag{34}$$

Based on the LaSalle's Invariance Principle [13], the proof indicated that the arbitrary initial error $[x_e, z_e]^{\mathrm{T}} \in \mathbb{R}^2$ can asymptotically converge to Ω_{nav}. The rest of proof showed that the largest invariant set Ω_{nav} can asymptotically converge to Ω_{path}. This indicates that the arbitrary initial error $[x_e, z_e]^T \in \mathbb{R}^2$ asymptotically converge to the origin. ■

To achieve high-quality tracking response and satisfactory differential performance from virtual desired control commands, the desired pitch angular velocity β_q is introduced to a

first order low-pass filter to obtain its derivative $\dot{\beta}_q$. The low-pass filter is employed as following on the basis of dynamic surface control:

$$\begin{cases} T_q\dot{\hat{\beta}}_q + \hat{\beta}_q = \beta_q \\ \hat{\beta}_q(0) = \beta_q(0) \end{cases} \tag{35}$$

where T_q is the positive filter time constant. From Eq. (35), the desired pitch angular acceleration $\dot{\beta}_q$ is

$$\dot{\hat{\beta}}_q = \frac{\beta_q - \hat{\beta}_q}{T_q} \tag{36}$$

The filtering error is defined as: $\tilde{\beta}_q = \hat{\beta}_q - \beta_q$.

B. THE SURGE VELOCITY GUIDANCE

To avoid set-point jump, the nonlinear tracking differentiator [13], [37], which can arrange the excessive process of the surge velocity of the vehicle. The tracking differentiator is provided as follows

$$\begin{cases} \dot{\beta}_u = \beta_{\dot{u}} \\ \dot{\beta}_{\dot{u}} = -\vartheta\, sgn(\beta_u - u_R + \dfrac{\beta_{\dot{u}}\,|\beta_{\dot{u}}|}{2\vartheta}) \end{cases} \tag{37}$$

where β_u and $\beta_{\dot{u}}$ are the desired surge velocity and acceleration, respectively. u_R is reference surge velocity and input signal to be differentiated. ϑ is the supremum or infimum of $\dot{\beta}_{\dot{u}}$, i.e., $|\dot{\beta}_{\dot{u}}| \le r$. The details of the tracking differentiator are shown in the literature [37].

IV. THE DYNAMIC CONTROLLER DESIGN

In this section, the bottom-following dynamic controller is divided into two subsystems, namely the surge velocity control and pitch control. To improve the bottom-following performance and convergence despite the uncertainties, the recursive sliding mode control is employed. Meanwhile, an anti-windup compensator is introduced to eliminate the influence of input saturation. The detailed designing and deriving process are presented as follows.

A. THE PITCH CONTROLLER DESIGN

Step1. The recursive sliding mode with the pitch angular velocity error $q_e = q - \hat{\beta}_q$ is defined as follows

$$S_2 = c_1^q S_1 + q_e \tag{38}$$

where c_1^q is positive definite parameter. The first derivative of the sliding surface S_2 is calculated as

$$\begin{aligned} \dot{S}_2 &= c_1^q \dot{S}_1 + \dot{q}_e \\ &= c_1^q \dot{S}_1 + ((m_{22} - m_{11})uw - M_q q - M_{q|q|} q\,|q| \\ &\quad - (z_G W - z_B B)\sin\theta + \tau_q^c + \Delta f_q)\Big/ m_{33} - \dot{\hat{\beta}}_q \end{aligned} \tag{39}$$

The RBF NN is introduced to approximate the model uncertainties Δf_q (including the parameter perturbation and unmodeled dynamics), that is

$$\Delta f_q = \hat{\boldsymbol{W}}_q^{\mathrm{T}} \boldsymbol{h}_q(q) + \Delta\tilde{f}_q \tag{40}$$

where, $\hat{\boldsymbol{W}}_q$ is the estimate of the ideal weight vector $\boldsymbol{W}_q^*$ and the updated law for $\hat{\boldsymbol{W}}_q$ is set to

$$\dot{\hat{\boldsymbol{W}}}_q = \Gamma_q(L(S_2)\boldsymbol{h}_q(q) - \sigma_q \hat{\boldsymbol{W}}_q) \tag{41}$$

where Γ_q and σ_q are adjustable positive gain parameters. $\Delta\hat{f}_q$ is the estimated value of the model uncertainties Δf_q, and $\Delta\tilde{f}_q = \Delta f_q - \Delta\hat{f}_q$. Consider the initial system errors, the approximation error and the external disturbances, the nonlinear reaching law is employed to this sliding mode control strategy

$$\dot{S}_2 = -\frac{c_2^q S_2 + k_2^q L(S_2) + L(S_1)\big/N(S_2) + \Xi_q\hat{\delta}_q}{m_{33}} \tag{42}$$

where c_2^q and k_2^q are adjustable positive gain parameters. Ξ_q is designed as follows

$$\Xi_q = \tanh(\frac{L(S_2)}{\zeta_q}) \tag{43}$$

where $\tanh(\cdot)$ is the hyperbolic tangent function. ζ_q is an adjustable positive gain parameter. The approximation error ε_q and the external disturbances τ_{qex} are bounded, that is $\left|\Delta\tilde{f}_q\right| + |\tau_{qex}| \le \delta_q$, where δ_q is bounded function. The adaptive updated law for $\hat{\delta}_q$ is designed as follows

$$\dot{\hat{\delta}}_q = \gamma_q(\Xi_q L(S_2) - \Lambda_q(\hat{\delta}_q - \delta_q^0)) \tag{44}$$

where γ_q and Λ_q are adjustable positive gain parameters. δ_q^0 is prior estimate δ_q (including the approximation error and the external disturbances). Then, the pitch dynamic controller is eventually designed as follows

$$\begin{aligned} \tau_q^c &= (m_{11} - m_{22})uw + M_q q + M_{q|q|} q\,|q| \\ &\quad + (z_G W - z_B B)\sin\theta + m_{33}\dot{\hat{\beta}}_q - c_1^q m_{33}\dot{S}_1 - \hat{\boldsymbol{W}}_q^{\mathrm{T}}\boldsymbol{h}_q(q) \\ &\quad - c_2^q S_2 - k_2^q L(S_2) - L(S_1)\big/N(S_2) - \Xi_q\hat{\delta}_q \end{aligned} \tag{45}$$

Remark 1: The hyperbolic tangent function Ξ_q is introduce to eliminate chattering. The term $N(S_2)$ is employed to eliminate coupling terms. $\hat{\delta}_q$ is applied to compensate neural network approximation error and external environment disturbance.

Step2. To compensate the saturation of the motion control actuators, the following anti-windup compensator is introduced to the pitch dynamic controller [39], that is

$$\dot{\chi}_q = \begin{cases} -\lambda_q\chi_q \\ \quad - \dfrac{|L(S_2)\Delta\tau_q| + 0.5(\Delta\tau_q)^2}{|\chi_q|^2}\chi_q + \Delta\tau_q, & |\chi_q| \ge l_q \\ 0, & |\chi_q| < l_q \end{cases} \tag{46}$$

where, λ_q is positive definite parameter. $\Delta\tau_q = \tau_q^c - \tau_q$.

Remark 2: In fact, the defined anti-windup compensator is an auxiliary design system used to reduce effects of the input saturation. Only when$\Delta\tau_q \ne 0$, the compensator is activated

to compensate the input error. Then, the constrained pitch dynamic controller is redesigned as

$$\begin{aligned}\tau_q = &(m_{11}-m_{22})uw + M_q q + M_{q|q|}q\,|q| \\ &+ (z_G W - z_B B)\sin\theta + m_{33}\dot{\hat{\beta}}_q - c_1^q m_{33}\dot{S}_1 - \hat{\boldsymbol{W}}_q^{\mathrm{T}}\boldsymbol{h}_q(q) \\ &- c_2^q S_2 - k_2^q L(S_2) - L(S_1)/N(S_2) - \Xi_q\hat{\delta}_q + b_q\chi_q\end{aligned} \tag{47}$$

where, b_q is positive definite parameter.

Theorem 2: Consider the dynamics of an underactuated UUV described in Eq. (3) and the attitude guidance (28). The pitch angular velocity error q_e under the pitch dynamic controller is guaranteed to converge to a specified compact set around the origin by appropriately tuning those design parameters, the solutions of the closed-loop system is uniformly ultimately bounded.

Proof: Taking into account of the pitch angle error, pitch angular velocity error, filtering error and the adaptive error of RBF NN, the following Lyapunov function candidate is chosen as follows

$$\begin{aligned}V_{dyn1} = &\frac{1}{2}S_1\varpi(S_1) + \frac{1}{2}m_{33}S_2\varpi(S_2) \\ &+ \frac{1}{2}\tilde{\boldsymbol{W}}_q^{\mathrm{T}}\Gamma_q^{-1}\tilde{\boldsymbol{W}}_q + \frac{1}{2}\gamma_q^{-1}\tilde{\delta}_q^2 + \frac{1}{2}\tilde{\beta}_q^2 + \frac{1}{2}\chi_q^2\end{aligned} \tag{48}$$

where, $\tilde{\boldsymbol{W}}_q = \hat{\boldsymbol{W}}_q - \boldsymbol{W}_q^*$ is the estimated error of the RBF NN weight vector, and $\tilde{\delta}_q = \hat{\delta}_q - \delta_q$ is the estimated error of the adaptive law. Calculating the time-derivative of the Lyapunov function (48), the result is obtain as follows:

$$\begin{aligned}\dot{V}_{dyn1} = &\dot{S}_1 L(S_1) + m_{33}\dot{S}_2 L(S_2) \\ &+ \tilde{\boldsymbol{W}}_q^{\mathrm{T}}\Gamma_q^{-1}\dot{\hat{\boldsymbol{W}}}_q + \gamma_q^{-1}\tilde{\delta}_q\dot{\tilde{\delta}}_q + \tilde{\beta}_q\dot{\tilde{\beta}}_q + \chi_q\dot{\chi}_q\end{aligned} \tag{49}$$

According to Eqs. (27), (28) and (38), $\dot{S}_1 L(S_1)$ can be obtained as follows:

$$\begin{aligned}\dot{S}_1 L(S_1) &= (q - \dot{\alpha} - \kappa(s)\dot{s} - \dot{\delta}_\theta)L(S_1) \\ &= (-k_1^q L(S_1) + S_2 - c_1^q S_1 + \tilde{\beta}_q)L(S_1)\end{aligned} \tag{50}$$

Consider the input saturation, the time-derivative of the sliding mode surface S_2 can be rewritten as follows:

$$\begin{aligned}\dot{S}_2 &= c_1^q\dot{S}_1 + \dot{q}_e \\ &= c_1^q\dot{S}_1 + ((m_{22}-m_{11})uw - M_q q - M_{q|q|}q\,|q| \\ &\quad - (z_G W - z_B B)\sin\theta + \tau_q + \Delta\tau_q + \Delta f_q)/m_{33} - \dot{\tilde{\beta}}_q\end{aligned} \tag{51}$$

According to Eq. (51) and (47), $\dot{S}_2 L(S_2)$ can be obtained as follows:

$$\begin{aligned}m_{33}\dot{S}_2 L(S_2) &= (\Delta f_q - \hat{\boldsymbol{W}}_q^{\mathrm{T}}\boldsymbol{h}_q(q) - c_2^q S_2 - k_2^q L(S_2) \\ &\quad - L(S_1)/N(S_2) - \Xi_q\hat{\delta}_q + b_q\chi_q + \Delta\tau_q)L(S_2) \\ &\le (-\tilde{\boldsymbol{W}}_q^{\mathrm{T}}\boldsymbol{h}_q(q) - c_2^q S_2 - k_2^q L(S_2) - L(S_1)/N(S_2) \\ &\quad - \Xi_q\hat{\delta}_q + \delta_q + b_q\chi_q + \Delta\tau_q)L(S_2)\end{aligned} \tag{52}$$

From Eq. (44), the result can be given as

$$\begin{aligned}\gamma_q^{-1}\tilde{\delta}_q\dot{\hat{\delta}}_q &= \gamma_q^{-1}\tilde{\delta}_q\gamma_q\left[\Xi_q L(S_2) - \Lambda_q(\hat{\delta}_q - \delta_q^0)\right] \\ &= \tilde{\delta}_q\Xi_q L(S_2) - \frac{\Lambda_q}{2}(\hat{\delta}_q - \delta_q)^2 - \frac{\Lambda_q}{2}(\hat{\delta}_q - \delta_q^0)^2 \\ &\quad + \frac{\Lambda_q}{2}(\delta_q - \delta_q^0)^2 \\ &\le \tilde{\delta}_q\Xi_q L(S_2) - \frac{\Lambda_q}{2}\gamma_q\tilde{\delta}_q\gamma_q^{-1}\tilde{\delta}_q + \frac{\Lambda_q}{2}(\delta_q - \delta_q^0)^2\end{aligned} \tag{53}$$

According to Eq. (36), the time-derivative of the filtering error $\tilde{\beta}_q$ is

$$\dot{\tilde{\beta}}_q = \dot{\hat{\beta}}_q - \dot{\beta}_q = -\frac{\tilde{\beta}_q}{T_q} - \ddot{\alpha} - \kappa(s)\ddot{s} - \dot{\kappa}(s)\dot{s} - \ddot{\delta}_\theta + k_1^q\dot{L}(S_1) \tag{54}$$

Consider two compact sets $\{\Pi_1|(S_1, \tilde{\beta}_q) \in \mathbb{R}^2, S_1^2 + \tilde{\beta}_q^2 < \Gamma\}$ and $\{\Pi_2|(\delta_\theta, \dot{\delta}_\theta, \ddot{\delta}_\theta) \in \mathbb{R}^3, |\delta_\theta|^2 + |\dot{\delta}_\theta|^2 + |\ddot{\delta}_\theta|^2 < I\}$, where Γ and I are the designed positive constants. Then, it is easily known that $\Pi_1 \times \Pi_2$ is also compact set, and there exists non-negative continuous function $\eta(\cdot)$ satisfies

$$\left\|\dot{\tilde{\beta}}_q + \frac{\tilde{\beta}_q}{T_q}\right\| \le \eta(S_1, \tilde{\beta}_q, \delta_\theta, \dot{\delta}_\theta, \ddot{\delta}_\theta) \tag{55}$$

and its maximum $\eta_{\max}$ within the compact set $\Pi_1 \times \Pi_2$ exists. Thus,

$$\tilde{\beta}_q\dot{\tilde{\beta}}_q = -\frac{\tilde{\beta}_q^2}{T_q} + \tilde{\beta}_q(\dot{\tilde{\beta}}_q + \frac{\tilde{\beta}_q}{T_q}) \le -\frac{\tilde{\beta}_q^2}{T_q} + \frac{\mu_q}{2}\tilde{\beta}_q^2 + \frac{\eta_{\max}^2}{2\mu_q} \tag{56}$$

where μ_q is a positive definite parameter. From Eq. (46), it is obtained as follows

$$\begin{aligned}\chi_q\dot{\chi}_q &= \chi_q(-\lambda_q\chi_q - \frac{|L(S_2)\Delta\tau_q| + 0.5(\Delta\tau_q)^2}{|\chi_q|^2}\chi_q + \Delta\tau_q) \\ &= -\lambda_q\chi_q^2 - |L(S_2)\Delta\tau_q| - 0.5(\Delta\tau_q)^2 + \chi_q\Delta\tau_q\end{aligned} \tag{57}$$

According Eq. (50) to Eq. (57), the time-derivative of the Lyapunov function V_{dyn1} can be rewritten as follows:

$$\begin{aligned}\dot{V}_{dyn1} \le &(-k_1^q L(S_1) + S_2 - c_1^q S_1 + \tilde{\beta}_q)L(S_1) \\ &+ (-\tilde{\boldsymbol{W}}_q^{\mathrm{T}}\boldsymbol{h}_q(q) - c_2^q S_2 - k_2^q L(S_2) - L(S_1)/N(S_2) \\ &- \Xi_q\hat{\delta}_q + \delta_q + b_q\chi_q + \Delta\tau_q)L(S_2) + \tilde{\boldsymbol{W}}_q^{\mathrm{T}}\Gamma_q^{-1}\dot{\hat{\boldsymbol{W}}}_q \\ &+ \tilde{\delta}_q\Xi_q L(S_2) - \frac{\Lambda_q}{2}\gamma_q\tilde{\delta}_q\gamma_q^{-1}\tilde{\delta}_q + \frac{\Lambda_q}{2}(\delta_q - \delta_q^0)^2 \\ &- \frac{\tilde{\beta}_q^2}{T_q} + \frac{\mu_q}{2}\tilde{\beta}_q^2 + \frac{\eta_{\max}^2}{2\mu_q} - \lambda_q\chi_q^2 - |L(S_2)\Delta\tau_q| \\ &- \frac{1}{2}(\Delta\tau_q)^2 + \chi_q\Delta\tau_q\end{aligned} \tag{58}$$

According to the nature of the hyperbolic tangent function, the following inequality holds

$$0 \le |A| - A\tanh(\frac{A}{\varepsilon}) \le 0.2785\varepsilon, \quad \forall\varepsilon > 0 \text{ and } \forall A \in \mathbb{R}$$

Thus, the following results can be obtained

$$\begin{aligned}&(-\Xi_q\hat{\delta}_q+\delta_q)L(S_2)+\tilde{\delta}_q\Xi_qL(S_2)\\&=(-\Xi_q\hat{\delta}_q+\delta_q)L(S_2)+(\hat{\delta}_q-\delta_q)\Xi_qL(S_2)\\&=\delta_q(L(S_2)-\Xi_qL(S_2))\le 0.2785\zeta_q\delta_q\end{aligned}\tag{59}$$

The following inequalities are obvious:

$$\begin{aligned}\Delta\tau_qL(S_2)&\le\left|\Delta\tau_qL(S_2)\right|,\quad \chi_q\Delta\tau_q\le\frac{1}{2}\chi_q^2+\frac{1}{2}\Delta\tau_q^2\\\tilde{\beta}_qL(S_1)&\le\frac{1}{2}L^2(S_1)+\frac{1}{2}\tilde{\beta}_q^2,\\b_q\chi_qL(S_2)&\le\frac{b_q}{2}L^2(S_2)+\frac{b_q}{2}\chi_q^2\\c_1^qS_1L(S_i)&\ge\frac{1}{2}c_1^qS_1\varpi(S_i)\quad(i=1,2),\\\sigma_q\tilde{\boldsymbol{W}}_q^{\mathrm{T}}\hat{\boldsymbol{W}}_q&\ge\frac{\sigma_q}{2}\left\|\tilde{\boldsymbol{W}}_q\right\|^2-\frac{\sigma_q}{2}\left\|\boldsymbol{W}_q^*\right\|^2\end{aligned}$$

Then, the time-derivative of the Lyapunov function V_{dyn1} satisfies

$$\begin{aligned}\dot{V}_{dyn1}\le&-\frac{c_1^q}{2}S_1\varpi(S_1)-\frac{c_2^q}{2}S_2\varpi(S_2)\\&-\frac{\Lambda_q}{2}\gamma_q\tilde{\delta}_q\gamma_q^{-1}\tilde{\delta}_q-\frac{\sigma_q}{2}(\left\|\tilde{\boldsymbol{W}}_q\right\|^2-\left\|\boldsymbol{W}_q^*\right\|^2)\\&+(\frac{1}{2}-\frac{1}{T_q}+\frac{\mu_q}{2})\tilde{\beta}_q^2+(\frac{1}{2}+\frac{b_q}{2}-\lambda_q)\chi_q^2\\&+(\frac{1}{2}-k_1^q)L^2(S_1)+(\frac{b_q}{2}-k_2^q)L^2(S_2)\\&+\frac{\Lambda_q}{2}(\delta_q-\delta_q^0)^2+0.2785\zeta_q\delta_q+\frac{\eta_{\max}^2}{2\mu_q}\end{aligned}\tag{60}$$

Let $2k_1^q=1$, $b_q=2k_2^q$, $2\lambda_q>b_q+1$ and $1+\mu_q<2/T_q$, Eq. (60) becomes as follows:

$$\begin{aligned}\dot{V}_{dyn1}\le&-\frac{c_1^q}{2}S_1\varpi(S_1)-\frac{c_2^q}{2m_{33}}m_{33}S_2\varpi(S_2)\\&-\frac{\sigma_q\Gamma_q}{2}\tilde{\boldsymbol{W}}_q^{\mathrm{T}}\Gamma_q^{-1}\tilde{\boldsymbol{W}}_q-\frac{\Lambda_q}{2}\gamma_q\tilde{\delta}_q\gamma_q^{-1}\tilde{\delta}_q\\&-(\frac{1}{T_q}-\frac{1+\mu_q}{2})\tilde{\beta}_q^2-\frac{2\lambda_q-b_q-1}{2}\chi_q^2\\&+\frac{\Lambda_q}{2}(\delta_q-\delta_q^0)^2+0.2785\zeta_q\delta_q\\&+\frac{\eta_{\max}^2}{2\mu_q}+\frac{\sigma_q}{2}\left\|\boldsymbol{W}_q^*\right\|^2\\\le&-\mu_qV_{dyn1}+C_q\end{aligned}\tag{61}$$

where,

$$\mu_q=\min\{c_1^q,\frac{c_2^q}{m_{33}},\sigma_q\Gamma_q,\Lambda_q\gamma_q,2(\frac{1}{T_q}-\frac{1+\mu_q}{2}),2\lambda_q-b_q-1\}$$

$$C_q=\frac{\Lambda_q}{2}(\delta_q-\delta_q^0)^2+0.2785\zeta_q\delta_q+\frac{\eta_{\max}^2}{2\mu_q}+\frac{\sigma_q}{2}\left\|\boldsymbol{W}_q^*\right\|^2$$

From Eq. (61), the result can be obtained as follows:

$$V_{dyn1}(t)\le\frac{C_q}{\mu_q}+(V_{dyn1}(0)-\frac{C_q}{\mu_q})e^{-\mu_qt}\tag{62}$$

where $V_{dyn1}(0)$ is the initial value of the Lyapunov function V_{dyn1}. From Eq. (62), the Lyapunov function V_{dyn1} is uniformly ultimately bounded. Then, it is known that S_1, S_2, $\boldsymbol{W}_q^*$, δ_q and $\tilde{\beta}_q$ are bounded. Moreover, the parameters can be chosen to ensure the attitude tracking error converge the origin. ■

B. THE SURGE CONTROLLER DESIGN

In this subsection, the control torque of propellers for an underactuated UUV to achieve the desired surge velocity u_{R} is calculated.

Step1. A Lyapunov function candidate with the surge velocity error $u_e=u-\beta_u$:

$$V_{dyn2}=\frac{1}{2}m_{11}u_e^2\tag{63}$$

Differentiating Eq. (63) along Eq. (3), the calculation result yields

$$\begin{aligned}\dot{V}_{dyn2}=(u-\beta_u)(&-m_{22}wq-X_uu\\&-X_{u|u|}u\left|u\right|+\tau_u^c+\Delta f_u-m_{11}\dot{\beta}_u)\end{aligned}\tag{64}$$

The RBF NN is introduced to approximate the model uncertainties Δf_u (including the parameter perturbation and unmodeled dynamics), that is

$$\Delta f_u=\hat{\boldsymbol{W}}_u^{\mathrm{T}}\boldsymbol{h}_u(u)+\Delta\tilde{f}_u\tag{65}$$

where, $\hat{\boldsymbol{W}}_u$ is the estimate of the ideal weight vector $\boldsymbol{W}_u^*$ and the updated law for $\hat{\boldsymbol{W}}_u$ is set to

$$\dot{\hat{\boldsymbol{W}}}_u=\Gamma_u(u_e\boldsymbol{h}_u(u)-\sigma_u\hat{\boldsymbol{W}}_u)\tag{66}$$

where Γ_u and σ_u are adjustable positive gain parameters. $\Delta\hat{f}_u$ is the estimated value of the model uncertainties Δf_u, and $\Delta\tilde{f}_u=\Delta f_u-\Delta\hat{f}_u$. The approximation error and the external disturbances are bounded, that is $\left|\Delta\tilde{f}_u\right|+|\tau_{uex}|\le\delta_u$, where δ_u is bounded function. The adaptive updated law for $\hat{\delta}_u$ is designed as follows

$$\dot{\hat{\delta}}_u=\gamma_u(u_e\Xi_u-\Lambda_u(\hat{\delta}_u-\delta_u^0))\tag{67}$$

where, γ_u and Λ_u are adjustable positive gain parameters. δ_u^0 is prior estimate δ_u

$$\Xi_u=\tanh(\frac{u_e}{\zeta_u})\tag{68}$$

where ζ_u is an adjustable positive gain parameter. The surge dynamic controller is designed as follows

$$\begin{aligned}\tau_u^c=m_{22}wq+X_uu+X_{u|u|}u\left|u\right|-\hat{\boldsymbol{W}}_u^{\mathrm{T}}\boldsymbol{h}_u(u)\\-\Xi_u\hat{\delta}_u+m_{11}\dot{\beta}_u-k_uu_e\end{aligned}\tag{69}$$

Step2: The following anti-windup compensator is introduced to eliminate the input saturation

$$\dot{\chi}_u=\begin{cases}-\lambda_u\chi_u\\-\dfrac{|u_e\Delta\tau_u|+0.5(\Delta\tau_u)^2}{|\chi_u|^2}\chi_u+\Delta\tau_u,&|\chi_u|\ge l_u\\0,&|\chi_u|<l_u\end{cases}\tag{70}$$

where, λ_u is positive definite parameter. $\Delta\tau_u=\tau_u^c-\tau_u$.

Remark 3: In fact, the defined anti-windup compensator is an auxiliary design system used to reduce effects of the input saturation. Only when $\Delta\tau_u \neq 0$, the compensator is activated to compensate the input error.

Then, the constrained pitch dynamic controller is redesigned as

$$\tau_u = m_{22}wq + X_u u + X_{u|u|}u\,|u| - \hat{\boldsymbol{W}}_u^{\mathrm{T}}\boldsymbol{h}_u(u) - \Xi_u\hat{\delta}_u + m_{11}\dot{\beta}_u - k_u u_e + b_u\chi_u \quad (71)$$

where, b_u is positive definite parameter.

Theorem 3: Consider the dynamics of an underactuated UUV described in Eq. (3) and the surge velocity guidance (37). The surge velocity error u_e under the surge dynamic controller is guaranteed to converge to a specified compact set around the origin by appropriately tuning those design parameters, the solutions of the closed-loop system is uniformly ultimately bounded.

Proof: The Lyapunov function candidate is chosen as follows

$$V_{dyn3} = \frac{1}{2}m_{11}u_e^2 + \frac{1}{2}\tilde{\boldsymbol{W}}_u^{\mathrm{T}}\Gamma_u^{-1}\tilde{\boldsymbol{W}}_u + \frac{1}{2}\chi_u^2 + \frac{1}{2}\gamma_u^{-1}\tilde{\delta}_u^2 \quad (72)$$

where, $\tilde{\boldsymbol{W}}_u = \hat{\boldsymbol{W}}_u - \boldsymbol{W}_u$ is the estimated error of the RBF NN weight vector, and $\tilde{\delta}_u = \hat{\delta}_u - \delta_u$ is the estimated error of the adaptive law. The first time-derivative can be calculated as

$$\begin{aligned}\dot{V}_{dyn3} &= m_{11}u_e\dot{u}_e + \tilde{\boldsymbol{W}}_u^{\mathrm{T}}\Gamma_u^{-1}\dot{\hat{\boldsymbol{W}}}_u + \chi_u\dot{\chi}_u + \gamma_u^{-1}\tilde{\delta}_u\dot{\hat{\delta}}_u \\ &= u_e(-m_{22}wq - X_u u - X_{u|u|}u\,|u| + \tau_u + \Delta\tau_q \\ &\quad + \Delta f_u - m_{11}\dot{\beta}_u) + \tilde{\boldsymbol{W}}_u^{\mathrm{T}}(u_e\boldsymbol{h}_u(u) - \sigma_u\hat{\boldsymbol{W}}_u) \\ &\quad + \chi_u(-\lambda_u\chi_u - \frac{|u_e\Delta\tau_u| + 0.5(\Delta\tau_u)^2}{|\chi_u|^2}\chi_u + \Delta\tau_u) \\ &\quad + \tilde{\delta}_u(u_e\Xi_u - \Lambda_u(\hat{\delta}_u - \delta_u^0)) \\ &= u_e(-k_u u_e + b_u\chi_u - \Xi_u\hat{\delta}_u + \delta_u + \Delta\tau_u) - \tilde{\boldsymbol{W}}_u^{\mathrm{T}}\sigma_u\hat{\boldsymbol{W}}_u \\ &\quad - \lambda_u\chi_u^2 - |u_e\Delta\tau_u| - 0.5(\Delta\tau_u)^2 + \chi_u\Delta\tau_u \\ &\quad + \tilde{\delta}_u(u_e\Xi_u - \Lambda_u(\hat{\delta}_u - \delta_u^0)) \end{aligned} \quad (73)$$

The following inequalities are obvious:

$$u_e\Delta\tau_u \leq |u_e\Delta\tau_u|, \quad b_u\chi_u u_e \leq \frac{b_u}{2}\chi_u^2 + \frac{b_u}{2}u_e^2,$$
$$\chi_u\Delta\tau_u \leq \frac{1}{2}\chi_u^2 + \frac{1}{2}\Delta\tau_u^2, \quad 2\tilde{\boldsymbol{W}}_u\hat{\boldsymbol{W}}_u \geq \left\|\tilde{\boldsymbol{W}}_u\right\|^2 - \left\|\boldsymbol{W}_u^*\right\|^2$$

Then, the time-derivative of the Lyapunov function V_{dyn3} satisfies

$$\begin{aligned}\dot{V}_{dyn3} \leq\ & -(k_u - \frac{b_u}{2})u_e^2 - \frac{\sigma_u}{2}\left\|\tilde{\boldsymbol{W}}_u\right\|^2 - \frac{2\lambda_u - b_u - 1}{2}\chi_u^2 \\ & - \frac{\Lambda_u}{2}\gamma_u\tilde{\delta}_u\gamma_u^{-1}\tilde{\delta}_u + \frac{\sigma_u}{2}\left\|\boldsymbol{W}_u^*\right\|^2 \\ & + \frac{\Lambda_u}{2}(\delta_u - \delta_u^0)^2 + 0.2785\zeta_u\delta_u \end{aligned} \quad (74)$$

Let $2k_u > b_u$ and $2\lambda_u > b_u + 1$, Eq. (74)becomes as follows:

$$\dot{V}_{dyn3} \leq -\mu_u V_{dyn3} + C_u \quad (75)$$

where,

$$\mu_u = \min\{2k_u - b_u, \sigma_u\Gamma_u, 2\lambda_u - b_u - 1, \Lambda_u\gamma_u\}$$
$$C_u = \frac{\sigma_u}{2}\left\|\boldsymbol{W}_u^*\right\|^2 + \frac{\Lambda_u}{2}(\delta_u - \delta_u^0)^2 + 0.2785\zeta_u\delta_u$$

From Eq.(75), the result can be obtained as follows:

$$V_{dyn3}(t) \leq \frac{C_u}{\mu_u} + (V_{dyn3}(0) - \frac{C_u}{\mu_u})e^{-\mu_u t} \quad (76)$$

where $V_{dyn3}(0)$ is the initial value of the Lyapunov function V_{dyn3}. From Eq.(76), the Lyapunov function V_{dyn3} is uniformly ultimately bounded. Then, it is known that $\boldsymbol{W}_u^*$ and δ_u are bounded. Moreover, the parameters can be chosen to ensure the surge velocity error converge the origin. ■

V. NUMERICAL SIMULATIONS

In this section, the numerical simulation results are presented to validate the effectiveness and robustness of the proposed bottom-following control strategy. The dynamic equations of underactuated UUVs are provided for this simulation by referring to [13], which is assumed that the vehicle is equipped with propellers to generate force and moments in the surge and pitch DOF. The action of the control laws have been simulated for a UUV of mass $m = 185$ kg, given by the following model parameters: $m_{11} = 215$ kg, $m_{22} = 265$ kg, $m_{33} = 80\ \mathrm{kg}\cdot\mathrm{m}^2$, $X_u = 70\ \mathrm{kg}\cdot\mathrm{s}^{-1}$, $X_{u|u|} = 100\ \mathrm{kg}\cdot\mathrm{m}^{-1}$, $Z_w = 100\ \mathrm{kg}\cdot\mathrm{s}^{-1}$, $Z_{w|w|} = 200\ \mathrm{kg}\cdot\mathrm{m}^{-1}$, $M_q = 50\ \mathrm{kg}\cdot\mathrm{m}^2\cdot\mathrm{s}^{-1}$, $M_{q|q|} = 100\ \mathrm{kg}\cdot\mathrm{m}^2$, $z_G = 0.01$ m, $z_G = -0.01$ m, $B = W = 1813kg{\cdot}\mathrm{m}/\mathrm{s}^2$. In the numerical simulation, the dynamic motion model of an underactuated UUV is added the $\pm 20\%$ parameter perturbation in all hydrodynamic coefficients. The external time-varying disturbances are set to

$$\begin{cases}\tau_{uex} = 0.5\sin(0.1t) + \cos(0.1t + \pi/4) \\ \tau_{wex} = 0.5\sin(0.1t) + \cos(0.1t + \pi/4) \\ \tau_{qex} = 0.5\sin(0.2t)\end{cases} \quad (77)$$

The unmodeled dynamics and parameter perturbation of this underactuated UUV are assumed to be

$$\begin{cases}\Delta f_u = -\tilde{m}_{22}wq - \tilde{X}_u u - \tilde{X}_{u|u|}u\,|u| + 10u^3 \\ \Delta f_w = \tilde{m}_{11}uq - \tilde{Z}_w w - \tilde{Z}_{w|w|}w\,|w| + 10w^3 \\ \Delta f_q = (\tilde{m}_{22} - \tilde{m}_{11})uw - \tilde{M}_q q - \tilde{M}_{q|q|}q\,|q| + 100q^3\end{cases} \quad (78)$$

where $\sim$ denote the parameter perturbation.

In this work, the saturation characteristic of the motion control actuators is set to $\tau_{u\max} = 700$ N, $\tau_{u\min} = 0$ N, $\tau_{q\max} = 100\ \mathrm{N}\cdot\mathrm{m}$, $\tau_{q\min} = -100\ \mathrm{N}\cdot\mathrm{m}$. The reference path is characterized by the curvilinear abscissa s and is expressed as follows:

$$x_{\mathrm{R}}(s) = \begin{cases}10\sin(0.05s) + s0 \leq s \leq 400 \\ s + 9400 \leq s \leq 800 \\ s + 9800 \leq s \leq 1070 \\ s + 91070 \leq s\end{cases} \quad (79)$$

$$z_{\mathrm{R}}(s) = \begin{cases} 0.1s0 \le s \le 400 \\ 2\sin(0.05s) + 38400 \le s \le 800 \\ -0.145s + 155800 \le s \le 1070 \\ 01070 \le s \end{cases} \tag{80}$$

In this numerical simulation, the initial linear and angular velocities are set to $u(0) = 0$m/s, $w(0) = 0$m/s and $q(0) = 0$rad/s. Meanwhile, the initial position and pitch angler is $x(0) = 0$ m, $z(0) = 0$ m and $\theta(0) = 0$ rad.

The gain coefficients of the designed bottom-following controller is set as follows: $k_\theta = 0.35$, $k_c = 2$, $k_s = 0.1$, $k_1^q = 0.5$, $k_2^q = 0.5$, $k_\theta = 0.35$, $\vartheta = 0.01$, $u_{\mathrm{R}} = 1$, $T_q = 0.1$, $c_1^q = 1$, $c_2^q = 1$, $\Gamma_q = 0.1$, $\sigma_q = 10$, $\zeta_q = 0.01$, $l_q = 0.0001$, $\alpha = 1$, $\wp = 1$, $\gamma_q = 500$, $\Lambda_q = 10^{-7}$, $\lambda_q = 1.5$, $b_q = 1$, $\delta_q^0 = 0.1$, $k_u = 1$, $\Gamma_u = 50$, $\sigma_u = 0.0001$, $\zeta_u = 0.01$, $l_u = 0.0001$, $\gamma_u = 500$, $\Lambda_u = 10^{-7}$, $\lambda_u = 1.2$, $b_u = 1$, $\delta_u^0 = 0.01$. The center μ_j of the Gaussian kernel function within the RBF NN is chosen from $[-0.3, 0.3]$, and the width σ_j of the Gaussian kernel function is 3. $m = 61$ indicates that there exist 61 node of hidden layers. The update laws of the RBF NN is designed as Eqs. (41) and (66).

We perform two cases in bottom following simulation:(a) the controller without considering input saturation is marked as Without SA in the simulation figures; (b) the controller including the auxiliary system is marked as With SA. The primary simulation results are provided in Figs. 2∼7 and demonstrate that the performance with our proposed control is reasonably good. Fig.2 shows that the proposed method (With SA) can force the UUV with uncertainties and unknown disturbances to converge to the desired bottom under the input constraints. Since the approach angle is introduced to design the bottom following controller, the dynamic performance of underactuated UUV in the initial tracking stage is effectively improved.

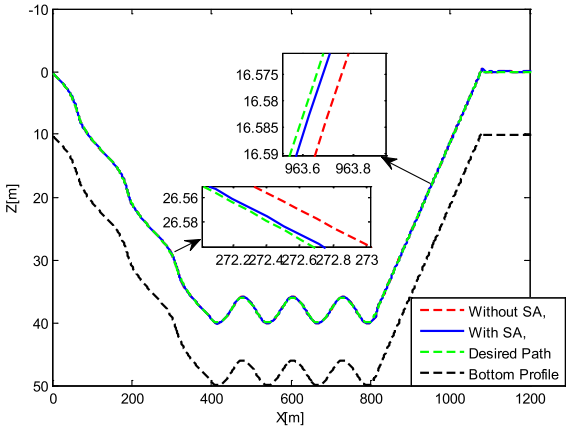

FIGURE 2. The bottom-following of underactuated UUV.

The bottom following errors are shown in Fig.3 with a small boundary, the designed controller (With SA) can guarantee the bottom following errors converge to zero and achieve precise bottom following control. Fig.4 shows the surge velocity response curve of underactuated UUV, from

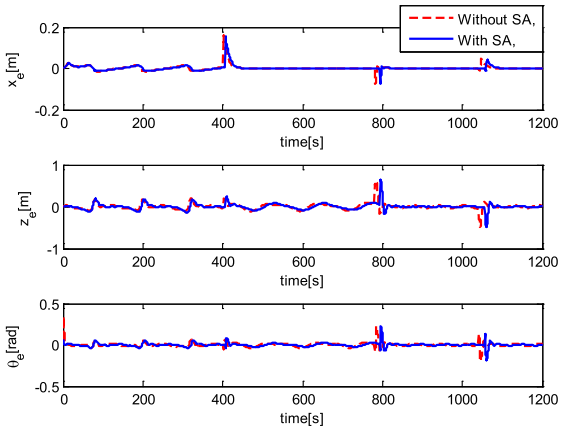

FIGURE 3. The position and pitch angler errors of the bottom-following for underactuated UUV.

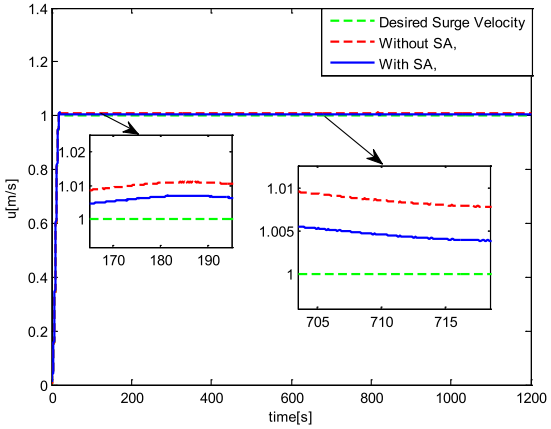

FIGURE 4. The surge velocity response of the underactuated UUV in the total simulation.

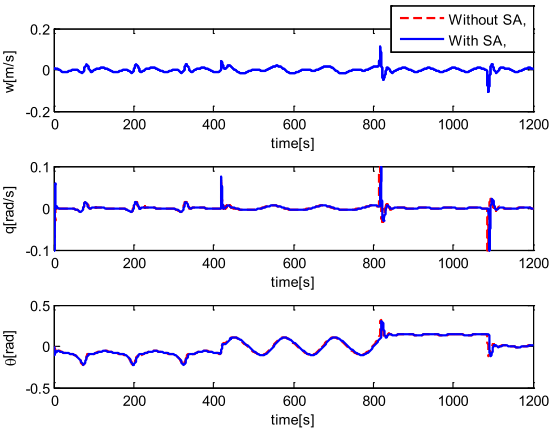

FIGURE 5. The heave velocity, the pitch angular velocity and the pitch angler response of the underactuated UUV in the total simulation.

which can be seen that the underactuated UUV can reach the desired surge velocity accurately under the action of the designed controller (With SA). Fig.5 presents the variation curves of heave velocity, pitch velocity and pitch angle of underactuated AUV. The heave velocity $w \le 0.1$m/s, which

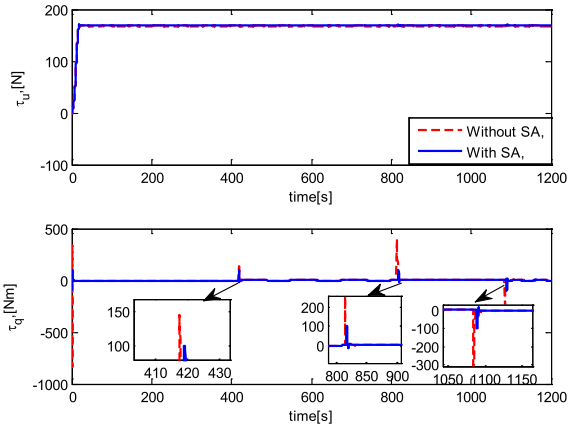

FIGURE 6. The surge force and pitch torque response of the underactuated UUV.

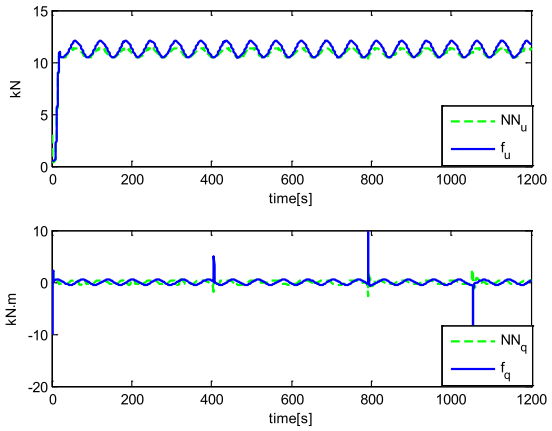

FIGURE 7. Estimates and actual of the multiple uncertainties.

is less than the surge velocity and guarantee the boundary of the surge velocity.

Fig.6 shows two control inputs curves. It can be observed that the proposed controllers (With SA) can solve the problem of actuator saturation. The inputs curve of the designed controller (With SA) is relatively stable, which further verifies the effectiveness of the design method in this paper. The control inputs of unconstrained controller (Without SA) are far beyond the operation condition of the actuators. This means that it is not practical. The estimated performance of the RBF neural network are shown in Fig.7. Based on the above simulation results, it can be seen that the proposed controller is more efficient and operable.

VI. CONCLUSION

This work propose a solution to the problem of the bottom-following control for underactuated UUVs with input saturation in the presence of unknown model uncertainties and unknown external disturbances. The bottom-following control scheme has been developed based on the recursive sliding mode with nonlinear gains and neural networks. The proposed control scheme achieves a balance between the feedback control gain and the system control performance due to introducing a novel nonlinear function featured by ''small-error large-gain and large-error small-gain'' into virtual and actual control laws. In addition, the ''explosion of terms'' problems in this work is overcome by dynamic surface control technique. By means of a newly constructed non-quadratic Lyapunov function, the theoretical analysis indicates that all signals in the closed-loop tracking control system are uniformly ultimately bounded. The simulation results validate the effectiveness and robustness of the proposed controller.

REFERENCES

[1] J. Yuh, ''Design and control of autonomous underwater robots: A survey,'' *Auton. Robots*, vol. 8, no. 1, pp. 7–24, 2000.

[2] F. Curado Teixeira, J. Quintas, and A. Pascoal, ''AUV terrain-aided navigation using a Doppler velocity logger,'' *Annu. Rev. Control*, vol. 42, pp. 166–176, Nov. 2016.

[3] J. Hwang, N. Bose, and S. Fan, ''AUV adaptive sampling methods: A review,'' *Appl. Sci.*, vol. 9, no. 15, p. 3145, Aug. 2019.

[4] A. Sahoo, S. K. Dwivedy, and P. S. Robi, ''Advancements in the field of autonomous underwater vehicle,'' *Ocean Eng.*, vol. 181, pp. 145–160, Jun. 2019.

[5] H. Yu, C. Guo, and Z. Yan, ''Globally finite-time stable three-dimensional trajectory-tracking control of underactuated UUVs,'' *Ocean Eng.*, vol. 189, Oct. 2019, Art. no. 106329.

[6] H. Yu, C. Guo, Z. Shen, and Z. Yan, ''Output feedback spatial trajectory tracking control of underactuated unmanned undersea vehicles,'' *IEEE Access*, vol. 8, pp. 42924–42936, 2020.

[7] T. I. Fossen, *Handbook of Marine Craft Hydrodynamics and Motion Control*. Chichester, U.K.: Wiley, 2011.

[8] A. P. Aguiar and J. P. Hespanha, ''Trajectory-tracking and path-following of underactuated autonomous vehicles with parametric modeling uncertainty,'' *IEEE Trans. Autom. Control*, vol. 52, no. 8, pp. 1362–1379, Aug. 2007.

[9] Z. Ma, J. Hu, J. Feng, and A. Liu, ''Diving adaptive position tracking control for underwater vehicles,'' *IEEE Access*, vol. 7, pp. 24602–24610, 2019.

[10] L. Qiao and W. Zhang, ''Trajectory tracking control of AUVs via adaptive fast nonsingular integral terminal sliding mode control,'' *IEEE Trans. Ind. Informat.*, vol. 16, no. 2, pp. 1248–1258, Feb. 2020.

[11] M. Mat-Noh, R. Mohd-Mokhtar, M. R. Arshad, Z. M. Zain, and Q. Khan, ''Review of sliding mode control application in autonomous underwater vehicles,'' *Indian J. Geo-Mar. Sci.*, vol. 48, no. 7, pp. 973–984, Jul. 2019.

[12] J. Rodriguez, H. Castañeda, and J. L. Gordillo, ''Design of an adaptive sliding mode control for a micro-AUV subject to water currents and parametric uncertainties,'' *J. Mar. Sci. Eng.*, vol. 7, no. 12, p. 445, Dec. 2019.

[13] Z.-P. Yan, H.-M. Yu, and B.-Y. Li, ''Bottom-following control for an underactuated unmanned undersea vehicle using integral-terminal sliding mode control,'' *J. Central South Univ.*, vol. 22, no. 11, pp. 4193–4204, Nov. 2015.

[14] H.-M. Jia, L.-J. Zhang, X.-Q. Bian, Z.-P. Yan, X.-Q. Cheng, and J.-J. Zhou, ''A nonlinear bottom-following controller for underactuated autonomous underwater vehicles,'' *J. Central South Univ.*, vol. 19, no. 5, pp. 1240–1248, May 2012.

[15] M. A. G. Rangel, A. Manzanilla, A. E. Z. Suarez, F. Muñoz, S. Salazar, and R. Lozano, ''Adaptive non-singular terminal sliding mode control for an unmanned underwater vehicle: Real-time experiments,'' *Int. J. Control, Autom. Syst.*, vol. 18, no. 3, pp. 615–628, Mar. 2020.

[16] X. Liu, M. Zhang, and S. Wang, ''Adaptive region tracking control with prescribed transient performance for autonomous underwater vehicle with thruster fault,'' *Ocean Eng.*, vol. 196, Jan. 2020, Art. no. 106804.

[17] L. Lapierre and B. Jouvencel, ''Robust nonlinear path-following control of an AUV,'' *IEEE J. Ocean. Eng.*, vol. 33, no. 2, pp. 89–102, Apr. 2008.

[18] K. Shojaei, ''Three-dimensional tracking control of autonomous underwater vehicles with limited torque and without velocity sensors,'' *Robotica*, vol. 36, no. 3, pp. 374–394, Mar. 2018.

[19] O. Elhaki and K. Shojaei, "A robust neural network approximation-based prescribed performance output-feedback controller for autonomous underwater vehicles with actuators saturation," *Eng. Appl. Artif. Intell.*, vol. 88, Feb. 2020, Art. no. 103382.
[20] O. Elhaki and K. Shojaei, "Neural network-based target tracking control of underactuated autonomous underwater vehicles with a prescribed performance," *Ocean Eng.*, vol. 167, pp. 239–256, Nov. 2018.
[21] X. Li and D. Zhu, "An adaptive SOM neural network method for distributed formation control of a group of AUVs," *IEEE Trans. Ind. Electron.*, vol. 65, no. 10, pp. 8260–8270, Oct. 2018.
[22] Z. Dong, T. Bao, M. Zheng, X. Yang, L. Song, and Y. Mao, "Heading control of unmanned marine vehicles based on an improved robust adaptive fuzzy neural network control algorithm," *IEEE Access*, vol. 7, pp. 9704–9713, 2019.
[23] K. Shojaei and M. Dolatshahi, "Line-of-sight target tracking control of underactuated autonomous underwater vehicles," *Ocean Eng.*, vol. 133, pp. 244–252, Mar. 2017.
[24] K. Shojaei, "Three-dimensional neural network tracking control of a moving target by underactuated autonomous underwater vehicles," *Neural Comput. Appl.*, vol. 31, no. 2, pp. 509–521, Feb. 2019.
[25] Z. Yan, Z. Yang, J. Zhang, J. Zhou, A. Jiang, and X. Du, "Trajectory tracking control of UUV based on backstepping sliding mode with fuzzy switching gain in diving plane," *IEEE Access*, vol. 7, pp. 166788–166795, 2019.
[26] B. Sun, D. Zhu, and S. X. Yang, "An optimized fuzzy control algorithm for three-dimensional AUV path planning," *Int. J. Fuzzy Syst.*, vol. 20, no. 2, pp. 597–610, Feb. 2018.
[27] C. Yu, X. Xiang, L. Lapierre, and Q. Zhang, "Nonlinear guidance and fuzzy control for three-dimensional path following of an underactuated autonomous underwater vehicle," *Ocean Eng.*, vol. 146, pp. 457–467, Dec. 2017.
[28] C. Silvestre, R. Cunha, N. Paulino, and A. Pascoal, "A bottom-following preview controller for autonomous underwater vehicles," *IEEE Trans. Control Syst. Technol.*, vol. 17, no. 2, pp. 257–266, Mar. 2009.
[29] A. Adhami-Mirhosseini, M. J. Yazdanpanah, and A. P. Aguiar, "Automatic bottom-following for underwater robotic vehicles," *Automatica*, vol. 50, no. 8, pp. 2155–2162, Aug. 2014.
[30] F. Li, C. Du, C. Yang, L. Wu, and W. Gui, "Finite-time asynchronous sliding mode control for Markovian jump systems," *Automatica*, vol. 109, Nov. 2019, Art. no. 108503.
[31] Z. Chu, F. Meng, D. Zhu, and C. Luo, "Fault reconstruction using a terminal sliding mode observer for a class of second-order MIMO uncertain nonlinear systems," *ISA Trans.*, vol. 97, pp. 67–75, Feb. 2020.
[32] C. Du, F. Li, and C. Yang, "An improved homogeneous polynomial approach for adaptive sliding-mode control of Markov jump systems with actuator faults," *IEEE Trans. Autom. Control*, vol. 65, no. 3, pp. 955–969, Mar. 2020.
[33] P. Sarhadi, A. R. Noei, and A. Khosravi, "Adaptive integral feedback controller for pitch and yaw channels of an AUV with actuator saturations," *ISA Trans.*, vol. 65, pp. 284–295, Nov. 2016.
[34] X. Liu, X. X. Sun, S. G. Liu, S. Xu, and Z. H. Cheng, "Recursive sliding-mode dynamic surface adaptive NN control with nonlinear gains," *Acta Autom. Sinica*, vol. 40, no. 10, pp. 2193–2202, Oct. 2014.
[35] Z. P. Shen and X. L. Zhang, "Recursive sliding-mode dynamic surface adaptive control for ship trajectory tracking with nonlinear gains," *Acta Autom. Sinica*, vol. 44, no. 10, pp. 1833–1841, Oct. 2018.
[36] C. Liu, C. L. P. Chen, Z. Zou, and T. Li, "Adaptive NN-DSC control design for path following of underactuated surface vessels with input saturation," *Neurocomputing*, vol. 267, pp. 466–474, Dec. 2017.
[37] J. Han, "From PID to active disturbance rejection control," *IEEE Trans. Ind. Electron.*, vol. 56, no. 3, pp. 900–906, Mar. 2009.
[38] A. Micaelli and C. Samson, "Trajectory tracking for two-steering-wheels mobile robots," *IFAC Proc. Volumes*, vol. 27, no. 14, pp. 249–256, Sep. 1994.
[39] R. Cui, X. Zhang, and D. Cui, "Adaptive sliding-mode attitude control for autonomous underwater vehicles with input nonlinearities," *Ocean Eng.*, vol. 123, pp. 45–54, Sep. 2016.

HAOMIAO YU was born in Harbin, China, in 1983. He received the B.S. degree in optical information science and engineering and the Ph.D. degree in control theory and control engineering from Harbin Engineering University, Harbin, China, in 2008 and 2016, respectively.

He is currently a Lecturer with the College of Marine Electrical Engineering, Dalian Maritime University, Dalian, China. His research interests include the design and development of navigation, and guidance and control algorithms for unmanned underwater vehicles and unmanned surface vehicles.

CHEN GUO was born in Dalian, China, in 1956. He received the B.E. degree from Chongqing University, Chongqing, China, in 1982, and the M.S. and Ph.D. degrees in marine engineering automation from Dalian Maritime University, Dalian, in 1985 and 1992, respectively.

He is currently a Professor with the College of Marine Electrical Engineering, Dalian Maritime University. His main activities are focused on intelligent control, soft computing, and marine system automation and simulation.

YANAN HAN received the B.S. degree in automation from the Harbin University of Science and Technology, Weihai, China, in 2017. She is currently pursuing the M.S. degree in control science and engineering with Dalian Maritime University, Dalian. Her research interests include under-actuated autonomous underwater vehicles, sliding mode control, back-stepping control, and active disturbance rejection control.

ZHIPENG SHEN was born in Fujian, China, in 1977. He received the B.E. and Ph.D. degrees in control engineering from Dalian Maritime University, Dalian, China, in 2000 and 2005, respectively. He is currently a Professor with the College of Marine Electrical Engineering, Dalian Maritime University. His research interests include nonlinear control, and intelligent control and its applications in surface vehicles.